STEM CELLS TRANSLATIONAL MEDICINE®

TISSUE ENGINEERING AND REGENERATIVE MEDICINE

Osteogenic Potential of Mouse Periosteum-Derived Cells Sorted for CD90 In Vitro and In Vivo

YOU-KYOUNG KIM, HIDEMI NAKATA, MAIKO YAMAMOTO, MUNEMITSU MIYASAKA, SHOHEI KASUGAI, SHINJI KURODA

Key Words. Periosteum • Periosteum-derived cell • CD90(+) • New bone formation • Three-dimensional cell migration

Department of Oral Implantology and Regenerative Dental Medicine, Division of Oral Health Sciences, Graduate School of Medical and Dental Sciences, Tokyo Medical and Dental University, Tokyo, Japan

Correspondence: Shinji Kuroda, D.D.S., Ph.D., Department of Oral Implantology and Regenerative Dental Medicine, Division of Oral Health Sciences, Graduate School of Medical and Dental Sciences, Tokyo Medical and Dental University, 1-5-45 Yushima, Bunkyo-ku, Tokyo 113-8510, Japan. Telephone: 81-03-5803-4656; E-Mail: skuroda.mfc@tmd.ac.jp

Received January 29, 2015; accepted for publication August 13, 2015; published Online First on December 30, 2015.

1066-5099/2015/$20.00/0

http://dx.doi.org/10.5966/sctm.2015-0013

ABSTRACT

The treatment of bone defects still presents complex problems, although various techniques have been developed. The periosteum is considered a good source of osteogenic precursor cells for new bone formation. It can be collected easily in the clinical setting and is less invasive to the donor site. However, the murine skull periosteum has a poor cellular component, and growth is very slow, making it important to identify a culture method for efficient growth. In the present study, we used three-dimensional cell migration with atelocollagen and gelatin media and found that both were effective for promoting the proliferation of periosteum-derived cells. Moreover, atelocollagen medium is expected to provide an added benefit as a scaffold structure in the ambient temperature of the human body. The selection of a proper surface marker for osteogenesis is imperative for bone regeneration. CD90 is a mesenchymal stem cell marker. Periosteum-derived cells sorted with CD90 showed higher proliferative capacity and osteogenic potential than that of unsorted periosteum-derived cells in vivo and in vitro. Thus, periosteum-derived cells sorted with CD90 are expected to be a good source for bone regeneration. STEM CELLS TRANSLATIONAL MEDICINE *2016;5:227–234*

SIGNIFICANCE

Periosteum-derived cells showed higher proliferative capacity and osteogenic potential. Periosteum can be collected easily in the clinical setting and is less invasive to the donor site. Thus, periosteum-derived cells can be expected to be a good source for bone regeneration.

INTRODUCTION

The periosteum is a fibrous tissue that covers the outside of the bone [1, 2]. It is divided into a fibrous and a cambium layer [3]. The fibrous layer on the outside of the periosteum contains fibroblasts in a collagen and elastin fiber matrix, along with a nerve and microvascular network [4, 5]. The cambium layer facing the bone consists of fibroblasts, osteoblasts, and a number of cellular components such as osteochondral precursor cells [6]. This is thought to be the layer responsible for producing osteoblasts and chondroblasts for bone formation or regeneration [7, 8]. The skull, clavicle, and part of the mandible are formed by intramembranous ossification, which begins on ossification of the periosteum during fetal development [9]. This fact supports the hypothesis that the periosteum might be related to bone growth and regeneration [10, 11]. Although many studies have used osteoblasts or bone marrow-derived mesenchymal stem or progenitor cells for bone regeneration and tissue engineering [12, 13], the osteogenic potential of periosteum-derived cells has not been examined in as many studies. However, the periosteum regenerative potential has become an intense topic in bone regeneration and tissue engineering [14]. Also, periosteum-derived cells can be acquired more easily and safely than bone marrow-derived mesenchymal stem or progenitor cells and by a less-invasive method. Thus, we supposed that periosteum-derived cells could emerge as a new source for bone tissue engineering.

The periosteum-derived cells contain a number of progenitor cell-related antigens such as SH2(+), SH3(+), SH4(+), CD9(+), CD90(+), and CD105(+) [15]. A few reports have demonstrated the ability of periosteum-derived cells to differentiate into chondrocytes and osteocytes [16]. CD90(+) is a glycosylphosphatidylinositol-anchored protein present in the lipid rafts of the cell surface [17]. It is expressed in osteoblast lineage cells and is believed to be involved in ossification [18]. Chung et al. reported that CD90(+) cells, sorted from adipose-derived

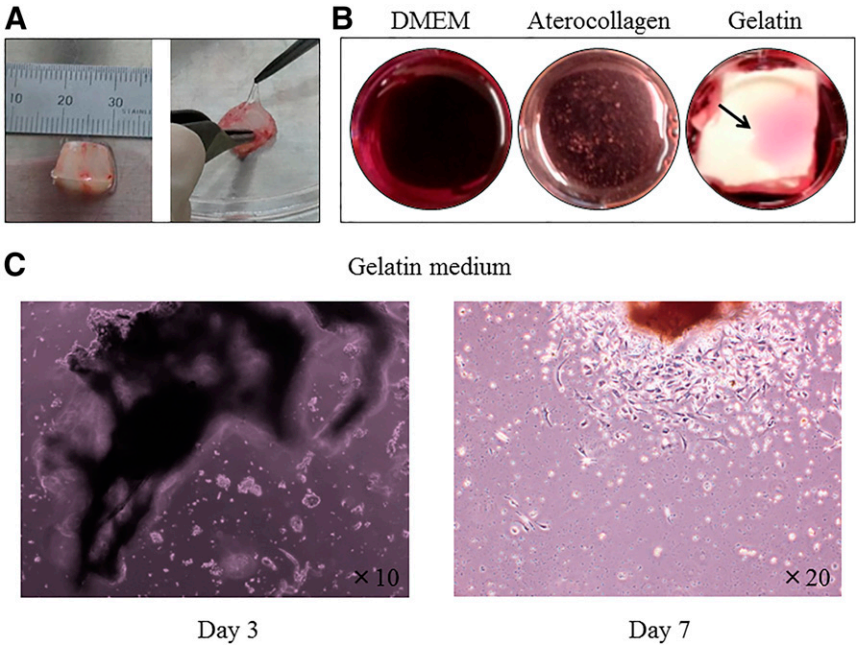

Figure 1. Two-dimensional cell culture in DMEM and three-dimensional cell migration in the atelocollagen and gelatin media. **(A):** Murine skull periosteum was trimmed to 10 × 10 mm^2. **(B):** Atelocollagen medium is not translucent, and gelatin medium, consisting of a white gelatin mass (black arrow), dissolves at 37°C. **(C):** Daughter cells from periosteum began to migrate down in the dishes by day 3, and the front cells had reached the bottom at day 7 in the gelatin medium. Abbreviation: DMEM, Dulbecco's modified Eagle's medium.

stromal cells, are more capable of enhancing bone formation both in vitro and in vivo [19]. Yamamoto et al., only from an in vitro study, described feasibility of the osteogenic potential of CD90(+) murine adipose-derived stem cells [20]. However, the role of CD90(+) in periosteum-derived cells remains unclear.

In the present study, the structure of murine periosteum was observed by histologic examination, and the osteogenic potential of CD90(+) periosteum-derived cells was investigated by transplantation into murine femoral medullae. We have also demonstrated a three-dimensional migration method for periosteum-derived cells.

Materials and Methods

The institutional animal care and use committee of Tokyo Medical and Dental University approved the protocol design and procedures (approval no. 0150221).

Three-Dimensional Cell Migration

Skulls with the periosteum from nine 4-week-old female ICR mice were collected after pentobarbital sodium euthanasia. After trimming the skulls to 10 × 10 mm^2 in size, the periosteum was peeled off the bone. Next, the samples were divided into three groups: atelocollagen group (CG), gelatin group (GG), and Dulbecco's modified Eagle's medium (DMEM) group (DG). In the CG, pieces of the periosteum were immersed in 2 ml of 0.2% atelocollagen medium (atelocollagen, Eagle's minimum essential medium; Koken Co., Ltd., Tokyo, Japan, http://www.kokenmpc.co.jp) on 6-well plates. In the GG, gelatin medium was used for the periosteum immersion in the same manner, which was manufactured by dissolving 0.4 g of gelatin (low endotoxin gelatin; Nippi Co., Yokohama, Japan, http://www.nippi.co.jp) gradually into 2 ml of DMEM (containing 4.5 g/l glucose and 0.584 g/l L-glutamine; Sigma-Aldrich, St. Louis, MO, http://sigmaaldrich.com) supplemented with 10% fetal bovine serum (FBS; Sigma-Aldrich) and 1% penicillin/streptomycin (Sigma-Aldrich), stirring them slowly at room temperature. The atelocollagen medium transforms into agar at 37°C, and the gelatin medium, which forms mushy, becomes aqueous at 37°C. The periosteum-derived cells of the CG and GG gradually migrated through the media and had landed on the plate surface by day 3 and started growing. In the last group, the DG, the periosteum was immediately digested into individual cells with 0.1% (wt/vol) collagenase (type I collagenase; Sigma-Aldrich) in 30 ml of phosphate-buffered saline (PBS; Wako Pure Chemical Industries, Ltd., Osaka, Japan, http://www.wako-chem.co.jp) by rocking for 10–15 minutes. The digested cells were plated on 6-well plates and cultured in 2 ml of DMEM supplemented with 10% FBS and 1% penicillin/streptomycin. All groups were continuously cultured at 37°C in a humidified atmosphere of 95% air and 5% CO_2 for 7 days.

Cell Viability

The atelocollagen and gelatin media were digested with collagenase to expose the periosteum-derived cells on the plates. The cells of the CG and GG were trypsinized (1% trypsin-EDTA; Sigma-Aldrich), centrifuged at 1,000*g* for 5 minutes in the presence of 1% FBS to quench the enzymes, and reseeded in 10 ml of DMEM on a 10-cm cell culture dish at an initial density of 2.5 × 10^2 cells per cm^2 for each. The DG was also passaged and reseeded on a 10-cm cell culture dish.

After 1 day of culture, all cells underwent viability measurement with PrestoBlue (PrestoBlue Cell Viability Reagent; Life Technologies, Carlsbad, CA, http://www.lifetechnologies.

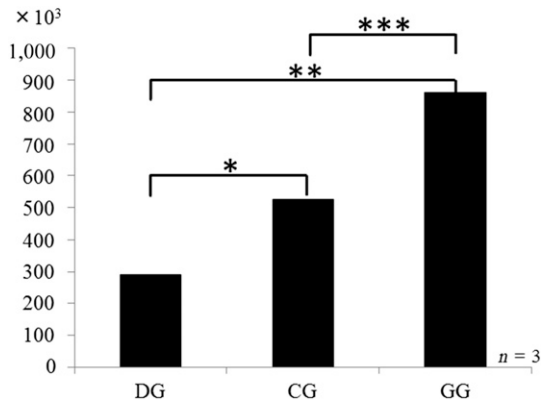

Figure 2. Cell viability stratified by fluorescence measurement. Relative fluorescence unit data were as follows: DG, 289029; CG, 525902; and GG, 861622. High cell proliferation was observed in the GG. Statistically significant differences were observed among the groups (*, $p < .05$; **, $p < .003$; ***, $p < .002$; $n = 3$). Abbreviations: CG, atelocollagen medium group; DG, Dulbecco's modified Eagle's medium group; GG, gelatin medium group.

com). PrestoBlue reagent was added to fresh culture medium at a volume ratio of 1:9 and incubated for 10 minutes at 37°C. Next, the reaction solution was transferred onto 96-well plates, 100 μl per well. Fluorescence was measured using a microplate reader (Perkin Elmer Wallac 1420 Victor 2 Microplate Reader; GMI, Ramsey, MN, http://www.gmi-inc.com) and quantified using a software program (Wallac 1420 workstation; PerkinElmer Life Sciences, Waltham, MA, http://www.perkinelmer.com).

Semiquantitative Polymerase Chain Reaction for Expression of Osteogenic Genes

The expression of genes associated with osteoblast differentiation in periosteum-derived cells was analyzed using polymerase chain reaction (PCR) with primer pairs designed using Primer3 software (http://bioinfo.ut.ee/primer3-0.4.0/). The primers used were as follows: runt-related transcription factor 2 (Runx2)—sense primer, 5′-tctggccttccactctcagt-3′; antisense primer, 5′-gactggcggggtgtaagtaa-3′; type I collagen—sense primer, 5′-tgctgttcttgggggactac-3′; antisense primer, 5′-gccatagaggggtgttctca-3′; Osterix (OSX)—sense primer, 5′-cccacctaacaggaggattt-3′; antisense primer, 5′-cactggaatggagtgaaacc-3′; and glyceraldehyde-3-phosphate dehydrogenase (GAPDH)—sense primer, 5′-acccagaagactgtggatgg-3′; antisense primer, 5′-cacattgggggtaggaacac-3′. Another set of periosteum-derived cells from the DG were pooled and homogenized in TRIzol reagent (Life Technologies) to extract total RNA. cDNA was synthesized using the SuperScript First-Strand Synthesis System for reverse transcription (RT)-PCR (Life Technologies). Real-time RT-PCR was performed on a 7300 real-time PCR system (Life Technologies), and target gene expression was normalized to GAPDH.

Mouse primary bone marrow cells were flushed from the femurs using a 27-gauge needle, pelleted quickly by centrifugation at 1,000*g* for 5 minutes, and washed with PBS. After centrifugation, the collected cells were cultured to confluence in 10 ml of DMEM supplemented with 10% FBS and 1% penicillin/streptomycin on a 10-cm culture dish. After being washed and supplied with fresh medium, the cells were trypsinized and reseeded on another 10-cm cell culture dish at the first passage and used as the control for RT-PCR analysis.

Histological Analysis

After collection from the skull of 8-week-old female ICR mice, the specimens were fixed with 10% neutralized formalin solution (Wako Pure Chemical Industries, Ltd.) for 2 weeks, decalcified in formic acid for 1 month, dehydrated, and embedded in paraffin. The periosteum without the skull was also harvested from another set of 8-week-old female ICR mice. The samples were fixed in 10% neutralized formalin solution for 2 days, dehydrated, and embedded in paraffin. For all samples, approximately 5-μm-thick coronal sections for histological examination were prepared, stained with hematoxylin and eosin (Sigma-Aldrich), and observed under an optical microscope (Biozero; Keyence, Tokyo, Japan, http://www.keyence.com).

Cell Sorting for CD90

The first passage of the periosteum-derived cells that had been cultured on a 10-cm dish was trypsinized (1% trypsin-EDTA; Sigma-Aldrich) and centrifuged at 1,000*g* for 5 minutes in the presence of 1% FBS to quench enzyme activity. The pellets were resuspended in 1% FBS in PBS, filtered through a 70-μm cell strainer (BD Biosciences, San Diego, CA, http://www.bdbiosciences.com), and the cells were counted using a One Cell Counter (Wako Pure Chemical Industries. Ltd.). The cells were separated into 100-μl fractions at a concentration of 1×10^7 cells per milliliter and then incubated at 4°C with 0.5 μg of anti-CD90/Thy1 FITC.MRC OX-7 per 1×10^6 cells (ab226; Abcam, Cambridge, U.K., http://www.abcam.com) for 40 minutes. Antibody-conjugated cells were filtered again through a 35-μm cell strainer (BD Biosciences). The cells were incubated with 5 μl of 7-amino-actinomycin D (7-AAD) staining solution (BD Biosciences) per 1×10^6 cells for 10 minutes and sorted by CD90 marker expression using fluorescence-activated cell sorting (FACS; FACSAria II; BD Biosciences). Cells emerging as CD90(+) were collected in DMEM supplemented with 1% penicillin/streptomycin and 10% FBS. Residual periosteum-derived cells, unsorted, were used as the control.

Viability of CD90(+) Periosteum-Derived Cells

To assess viability, the CD90(+) cells sorted by FACS were seeded on 24-well plates at an initial density of 2×10^2 cells per well. They were then cultured for up to 16 days in normal DMEM with 10% FBS and 1% penicillin/streptomycin or in an osteogenic medium supplemented with 10^{-8} M dexamethasone, 10 mM β-glycerophosphate, and 50 ng/ml ascorbic acid in DMEM. Unsorted periosteum-derived cells were also cultured in the same way. Viability was measured with the PrestoBlue reagents on days 1, 4, 7, 10, 13, and 16.

Alkaline Phosphatase-Positive CD90(+) Cell Staining

CD90(+) cells were seeded onto 6-well plates at an initial density of 5×10^2 cells/well in the normal DMEM or in the osteogenic medium. Naphthol AS-MX phosphatase (0.1 mg/ml) and Fast Blue BB Salt (0.6 mg/ml) were dissolved in Tris-HCl buffer (0.1 M; pH 8.8) containing 0.5% N,N-dimethylformamide and 2 mM $MgCl_2$. The solution was then filtered and used for alkaline phosphatase (ALP) staining (Sigma-Aldrich). Cells grown for 7, 14, and 21 days were washed twice with PBS and fixed in 10% formalin for 10 minutes. The fixed cells were rinsed twice with PBS and incubated in 1 ml of staining solution at 37°C for 20 minutes to develop the blue staining for ALP-positive cells. All cells were washed with

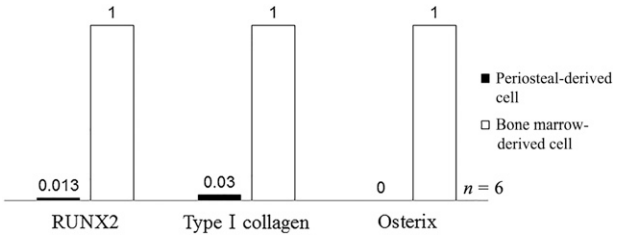

Figure 3. Reverse transcription-polymerase chain reaction. Semiquantified expression of type 1 collagen and RUNX2 in periosteum-derived cells was much lower than that in bone marrow-derived cells. Osterix was not detected (n = 6). Abbreviation: RUNX2, runt-related transcription factor 2.

PBS to stop the staining reaction. Unsorted periosteum-derived cells were also examined.

Alizarin Red Staining in CD90(+) Cell Culture

Another set of six-well plates was subjected for mineralized-nodule staining (alizarin red S staining). Mineralized nodules were stained after 7, 14, and 21 days of culture in another set of wells. The staining solution was prepared by dissolving alizarin red S (1%) in 1:100 aluminum hydroxide in water, followed by filtration. The cells were washed twice with PBS and immersed in methanol for 10 minutes. After rinsing in water, the cells were incubated with 500 μl of alizarin red S per well for 2 minutes until the mineralized nodules were stained red. The reactions were terminated by washing with water to remove excessive staining precipitate and reagents. Unsorted periosteum-derived cells were also tested.

Animal Experiment

To confirm the osteogenic ability of the periosteum-derived cells, the cells were transplanted into the femoral cavities of 8-week-old female ICR mice under ketamine anesthesia (100 mg/kg body weight) by intraperitoneal administration. An incision was made to expose the femoral knee joint. The femoral medulla was abraded through the epiphyseal plate from a femoral condyle and washed along the axis with normal saline using a 23-gauge needle (Terumo, Tokyo, Japan, http://www.terumo.com). The mice were divided into four groups: the first group was used as a sham control with no transplantation (saline group); the second group received a 0.3-ml injection of atelocollagen medium without cells (atelocollagen group); the third group was injected with 2×10^4 periosteum-derived cells in 0.3 ml of atelocollagen medium (periosteum group); and the fourth group received the same number of CD90(+) periosteum-derived cells in 0.3 ml of atelocollagen medium into the cavity [CD90(+) group]. After 3 weeks, the mice were euthanized, and paraffin-embedded sections of the femur were prepared for histologic examination by hematoxylin and eosin staining.

Statistical Analysis

Statistical analyses were performed using SPSS, version 14.0, for Windows (SPSS Inc., Chicago, IL, http://www.ibm.com). Differences between the means were analyzed using Student's t test. Data were considered statistically significant at $p \leq .05$.

RESULTS

Periosteum-Derived Cell Proliferation in Both Atelocollagen and Gelatin Media

The periosteum was dissected into 10-mm by 10-mm sections (Fig. 1A). Three-dimensional cell migration with an atelocollagen or gelatin medium as a scaffold was used to assess cell growth (Fig. 1B). Because of the ability of gelatin to turn more aqueous at 37°C, close to the inside body temperature of humans, migration and spreading of the daughter cells were observed in the gelatin medium. The front cells had reached the dish bottom by day 3, and their proliferation had begun by day 7 (Fig. 1C). Because the atelocollagen medium was not translucent, the cells in the atelocollagen were difficult to visualize and monitor.

Three-Dimensional Induction of Atelocollagen and Gelatin Media to Promote Growth of Periosteum-Derived Cells

To confirm the effect of the medium on cell growth, fluorescence measurement with PrestoBlue was performed (Fig. 2). The relative fluorescence unit data were as follows: DG, 289029; CG, 525902; and GG, 861622. CG proliferation was significantly higher versus the DG ($p < .05$), and the GG exhibited more efficient cell proliferation than the CG ($p < .003$) and the DG ($p < .002$). Statistically significant differences were observed between each group. Thus, three-dimensional migration in atelocollagen or gelatin medium was more effective than that in conventional two-dimensional culture for periosteum-derived cells. Atelocollagen and gelatin could serve as a scaffold to promote the proliferative activity of periosteum-derived cells. The differences in cell proliferation between the collagen and gelatin media might have resulted from differences in the structure. Collagen solidifies with increasing temperature, and gelatin melts as the temperature increases.

Bone Regeneration Potential of Periosteum-Derived Cells

Periosteum-derived cells were compared with bone marrow-derived cells for their osteogenic potential. Quantitative PCR was used to assess Runx2, OSX, and collagen type 1 expression (Fig. 3). Collagen type 1 and Runx2 were expressed in periosteum-derived cells, although OSX was not detected. The expression levels in the periosteum-derived cells were lower than those in the bone marrow-derived cells. Therefore, periosteum-derived cells are not mature osteoblasts but might have the potential to differentiate into osteoblasts.

Cells in the Cambium Layer

The structure of the murine skull periosteum was observed by hematoxylin and eosin staining (Fig. 4). The murine skull periosteum is a very thin tissue and is cell poor. Most of the cells were observed in the cambium layer.

Different Growth Rates and Patterns Between Unsorted Periosteum-Derived Cells and CD90(+) Cells

FACS was used to separate the periosteum-derived cells into a CD90(+) group and an unsorted group (Fig. 5A). During this process, the nonviable cells were eliminated using a cell viability assay (7-AAD cell viability assay kit; Life Technologies). All sorted CD90(+) cells survived in continuous culture for the experimental period of 12 days. Figure 5B is an electron microscopic image of unsorted periosteum-derived cells and CD90(+) cells after 3 and 12 days of culture. The images show the discrepancy in the growth rate and pattern of unsorted periosteum-derived cells and CD90(+) cells. The growth rate of the CD90(+) cells was greater than that of the unsorted periosteum-derived cells. Moreover, differences in the growth pattern between both groups were observed. The unsorted

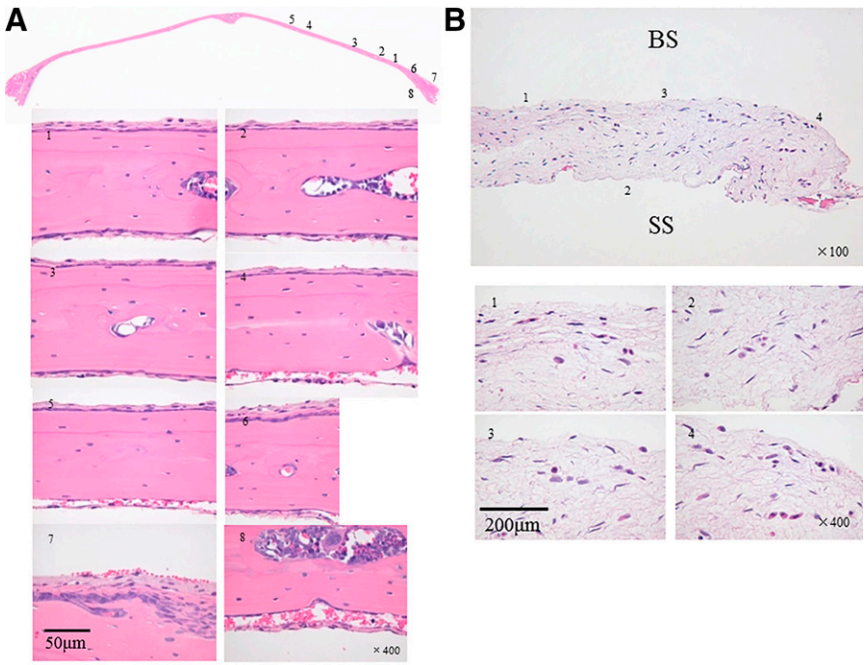

Figure 4. Hematoxylin and eosin staining of skull periosteum. Structure of the periosteum differs by site. Many of cellular components lie in the cambial layer. **(A):** Bone with periosteum. **(B):** Periosteum only. Abbreviations: BB, bone side; SB, skin side.

periosteum-derived cells grew in a star pattern and were condensed into small round cells after 3 days of culture. Many of the round cells resembled stars by day 12. In contrast, the CD90(+) cells were spindle-shaped cells in small round cells after 3 days of culture. These spindle-shaped cells were arranged in a column by day 12.

Osteogenic Potential and Proliferative Capacity of CD90(+) Cells

ALP staining and alizarin red staining were performed to examine the differences in osteogenic potential between the unsorted periosteum-derived cells and CD90(+) cells (Fig. 6A, 6B). The cells were cultured in DMEM and osteogenic medium for 1, 2, and 3 weeks. Over time, ALP activity and the number of mineralized nodules became higher, and the CD90(+) cells exhibited higher ALP activity than that of the unsorted periosteum-derived cells. In addition, the mineralized nodules were larger. The PrestoBlue cell viability assay showed that the proliferative ability of CD90(+) cells was greater than that of the unsorted periosteum-derived cells after 10 days of culture (Fig. 6C).

Bone Regeneration by Periosteum-Derived Cells in Femoral Marrow Cavity

To compare the bone regeneration ability of CD90(+) and unsorted periosteum-derived cells, a bone defect was created in the diaphysis through the epiphyseal plate of the femur (Fig. 7). Although condyle regeneration was prominent, the epiphyseal plate and the diaphysis had not been fully regenerated in the saline group (Fig. 7A). The atelocollagen group also showed findings similar to those in the saline group (Fig. 7B). Because the atelocollagen medium had gelled in the body, it prevented overflow of the medium and the cells out of the cavity. In the periosteum group, the epiphyseal plate and the diaphysis had healed more than in the saline and atelocollagen groups, although the regeneration seen in the diaphysis was not exaggerated (Fig. 7C). In contrast, mature regeneration of the diaphysis and the epiphyseal plate (Fig. 7D) was observed in the CD90(+) group. The epiphyseal plate in the CD90(+) group was similar to that of intact tissue (Fig. 7D, 7E). In summary, CD90(+) cells have the ability for bone regeneration with epiphyseal cartilage regeneration in vivo.

Discussion

Many studies have reported that the periosteum is a good source of osteogenic precursor cells for new bone formation [21–23]. Furthermore, the murine skull periosteum does not adhere to muscle or skin, such that the periosteum can be more easily collected. Thus, it was possible to isolate cells without the contamination of cells from a different origin. However, the murine skull periosteum has a poor cellular component, and growth is very slow. Therefore, a large number of mice will be required for experiments requiring a great number of cells. Thus, it is important to use a culture method that enhances cell growth. Wang et al. reported that the periosteum differs in composition and structure by site [24, 25]. The sites that receive more stress will have many cells, and the sites that receive less stress will contain fewer cellular components. We believe that the murine skull is cell poor, because it is not stressed. In the present study, three-dimensional culture systems with atelocollagen or gelatin medium were used to evaluate cell growth. Three-dimensional cell migration was effective in the atelocollagen and gelatin media, which became a scaffold for the periosteum-derived cells. Collagen is a component of extracellular matrices and is thought to aid in the growth and maturation of cells during culture [10]. Collagen has a triple-helical structure formed by three polypeptide chains. Collagen

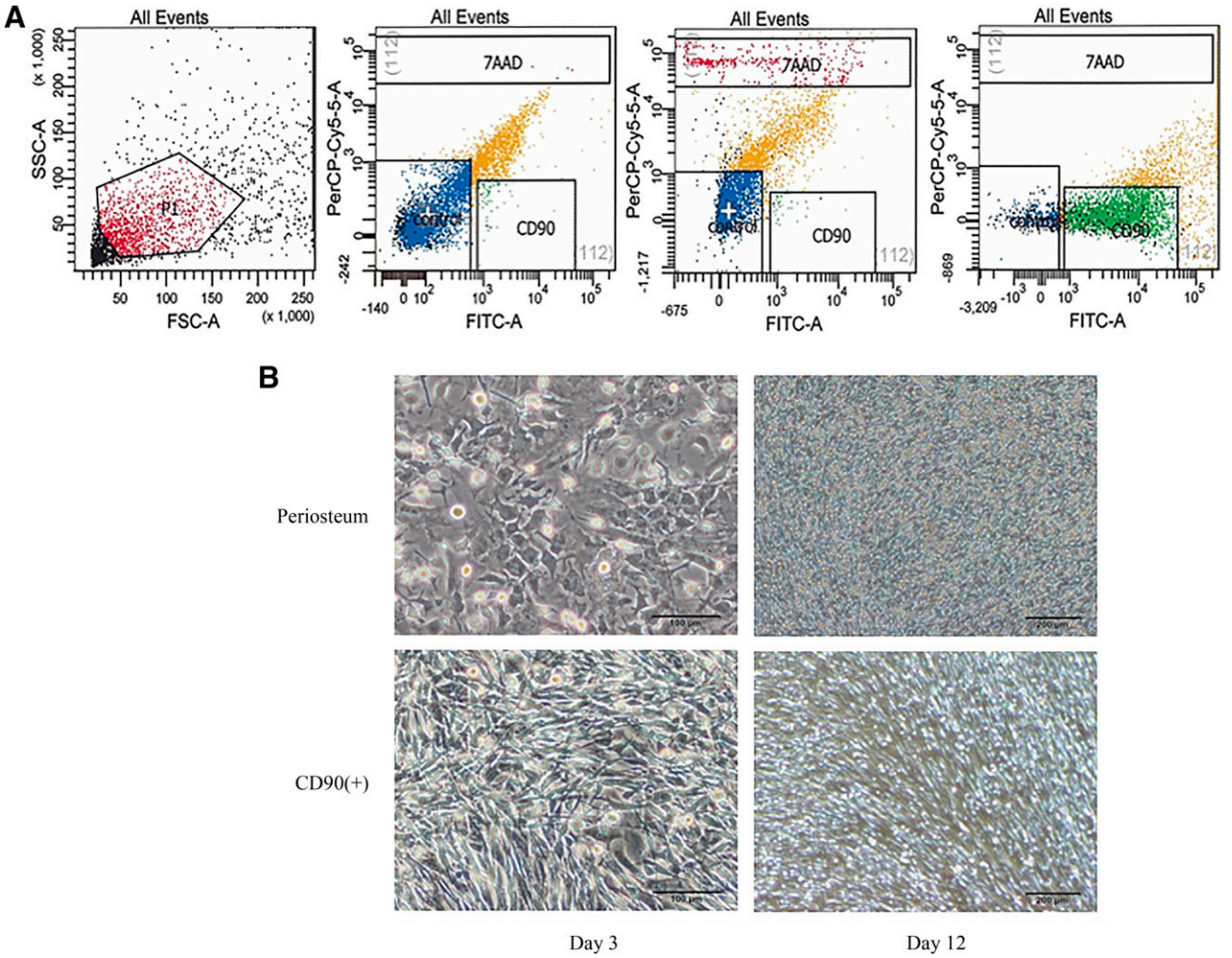

Figure 5. CD90 sorting by fluorescence-activated cell sorting. **(A):** Gate for CD90 and 7AAD. **(B):** Comparison between unsorted periosteum-derived cells (periosteum group) and CD90(+) periosteum-derived cells [CD90(+) group] at days 3 and 12. The growth rate of the CD90(+) group was faster than that of the periosteum group at day 3. The growth patterns differed in both groups. The periosteum group phenotypically expressed double aspects of a star-like shape and a round shape at day 3, and most cells in the periosteum group were round by day 12. In contrast, the CD90(+) group showed mostly spindle-shaped cells with scattered small round cells at day 3. These spindle-shaped cells occupied the culture area, aligning like a stream at day 12. Scale bar = 100 μm in day 3 panels and 200 μm in day 12 panels. Abbreviation: 7AAD, 7-amino-actinomycin D.

liquefies when cooled and solidifies when heated. These properties make three-dimensional cell migration possible at 37°C. Furthermore, collagen is expected to become a gel when injected into the body and can thereby serve as a scaffold. Gelatin is obtained by heat from collagen. With heat, the triple-helical structure of collagen changes to a random coiled structure, resulting in the formation of gelatin. As a result, gelatin possesses opposing characteristics. Thus, aqueous gelatin colloidal solution can be melted by heating and solidifies into a gel on cooling. Moreover, the firmness can be adjusted by changing the water-to-gelatin ratio. Because the gelatin will become a liquid in the body, it cannot be expected to serve as the scaffold. In the present study, the difference in cell proliferation in atelocollagen and gelatin media was likely associated with differences in the atelocollagen and gelatin structure. Atelocollagen solidifies with increasing temperature, but gelatin melts as the temperature increases. Therefore, gelatin medium secures the cell proliferation space, permitting high cell proliferation in culture conditions. The gelatin medium provided greater cell proliferation than did the atelocollagen medium, but it cannot be expected to serve as a scaffold as can atelocollagen medium.

The treatment of bone defects still presents complex problems, although various techniques have been developed [26–28]. Our data suggest that periosteum-derived cells also have osteogenic potential. For bone regeneration, the selection of a proper surface marker for osteogenesis is imperative [29–31]. CD90 is a mesenchymal stem cell marker [32, 33] and a member of the Ig supergene family, with structural similarity to the Ig VH region domain [34–36]. It allows cells to become multipotent and facilitates osteogenesis [37–39]. Chung et al. reported that CD90(+) cells have strong osteogenic capacity in vitro and in vivo [19]. In the present study, the CD90(+) periosteum-derived cells showed strong osteogenic potential. Chen et al. reported the highest level of constitutive expression of CD90(+) on proliferating cells; the expression decreased once the cells had progressed through the matrix maturation and mineralization stages [40]. Similarly, in the present study, ALP activity was increased in CD90(+) cells. The CD90(+)

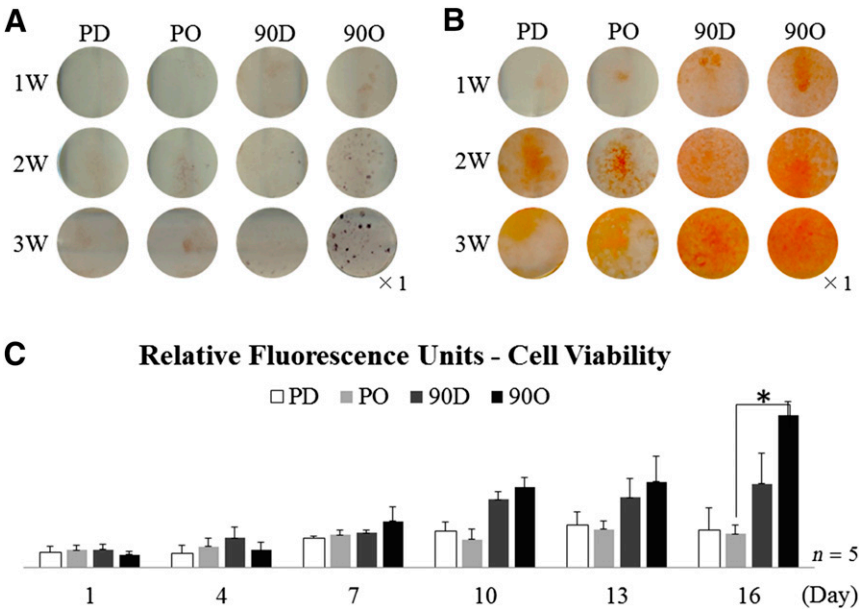

Figure 6. Alkaline phosphatase (ALP) activity, mineralized nodule formation, and cell viability. **(A):** ALP Staining. **(B):** Alizarin red S staining. In all cells, ALP activity and mineralized nodules became higher with time. 90D and 90O exhibited higher ALP activity and more mineral accumulation than did PD and PO. **(C):** Cell viability stratified by fluorescence measurement. The proliferative ability of 90D and 90O was greater than that of PD and PO after 10 days of culture. Statistically significant differences were observed between PO and 90O at day 16 (*, $p < .027$; $n = 5$). Abbreviations: 90D, CD90(+) cells in Dulbecco's modified Eagle's medium; 90O, CD90(+) cells in osteogenic medium; PD, periosteum-derived cells in Dulbecco's modified Eagle's medium; PO, periosteum-derived cells in osteogenic medium; W, week.

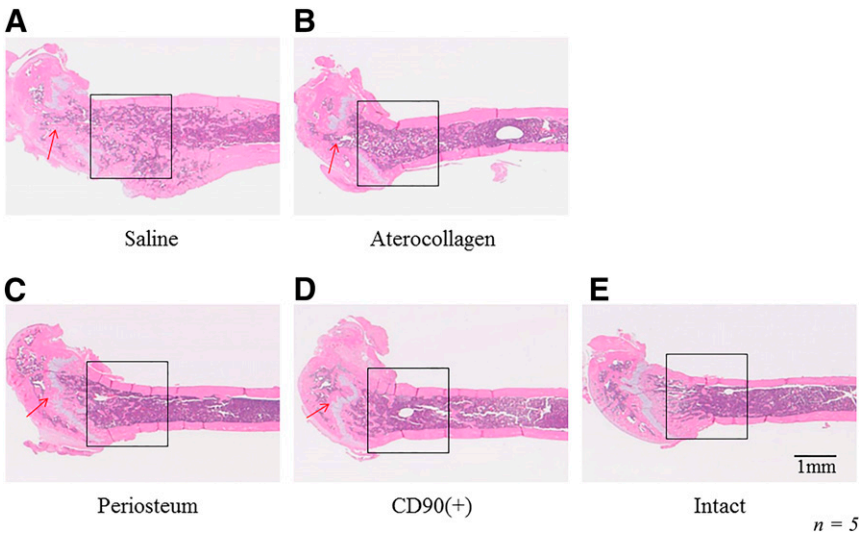

Figure 7. Histological analysis. The defect was created with a 23-guage needle in the femur ($n = 5$). **(A):** Saline group. **(B):** Atelocollagen group. **(C):** Periosteum group. **(D):** CD90(+) cell group. **(E):** Intact bone. Red arrow indicates the epiphyseal plate, and black box, the diaphysis in the defect site. In **(A)** and **(B)**, the epiphyseal plate and diaphysis had not been fully regenerated, although the condyle regeneration was prominent. The epiphyseal plate and diaphysis had almost healed in **(C)**. In particular, the CD90(+) groups had mature bone healing with regeneration of the condyle and epiphyseal **(D)**.

periosteum-derived cells showed strong proliferation and osteogenesis in vivo and in vitro and are expected to be a good source for bone regeneration.

Several minimum criteria have been proposed for human bone marrow-derived mesenchymal stem and progenitor cells: CD73, CD90, and CD105 expression positive and CD31, CD34, and CD45 expression negative in culture [41]. They have the ability to differentiate into adipocytes, chondrocytes, and osteocytes. In the present study, we assessed CD90 expression in periosteum-derived cells for osteogenic potential. The cells were initially not good at propagation on flat plates but were aggressive in the two groups with three-dimensional cell migration. Therefore, this strategy was used to expand the cell numbers for the subsequent analyses. Furthermore, recognition of three-dimensional cell migration of the periosteum cells could elicit a novel idea for effective bone regeneration. In our next study, we will explore the periosteum-derived cells for other mesenchymal stem cell markers.

Conclusion

Three-dimensional cell migration with atelocollagen and gelatin media promoted cell growth. Atelocollagen, which solidifies with increasing temperature, is a candidate for use as a scaffold. CD90(+) periosteum-derived cells showed strong proliferation and osteogenesis capacity in vivo and in vitro and are expected to be a good source for bone regeneration.

Acknowledgment

We acknowledge Dr. Michiko Suzuki, a Research Assistant in the Department of Oral Implantology and Regenerative Dental Medicine, Tokyo Medical and Dental University, Tokyo, Japan, for technical advice.

Author Contributions

Y.-K.K.: conception and design, collection and/or assembly of data, data analysis and interpretation, manuscript writing; H.N.: conception and design, financial support, provision of study material or patients; M.Y. and M.M.: data analysis and interpretation; S. Kasugai: final approval of manuscript; S. Kuroda: conception and design, financial support, provision of study material or patients, final approval of manuscript.

Disclosure of Potential Conflicts of Interest

S. Kuroda has uncompensated research funding from Japan Society for the Promotion of Science. The other authors indicated no potential conflicts of interest.

References

1 Ball MD, Bonzani IC, Bovis MJ et al. Human periosteum is a source of cells for orthopaedic tissue engineering: A pilot study. Clin Orthop Relat Res 2011;469:3085–3093.
2 Allen MR, Hock JM, Burr DB. Periosteum: Biology, regulation, and response to osteoporosis therapies. Bone 2004;35:1003–1012.
3 Ellender G, Feik SA, Carach BJ. Periosteal structure and development in a rat caudal vertebra. J Anat 1988;158:173–187.
4 Malizos KN, Papatheodorou LK. The healing potential of the periosteum molecular aspects. Injury 2005;36(suppl 3):S13–S19.
5 Hohmann EL, Elde RP, Rysavy JA et al. Innervation of periosteum and bone by sympathetic vasoactive intestinal peptide-containing nerve fibers. Science 1986;232:868–871.
6 Youn I, Suh JK, Nauman EA et al. Differential phenotypic characteristics of heterogeneous cell population in the rabbit periosteum. Acta Orthop 2005;76:442–450.
7 Ito Y, Fitzsimmons JS, Sanyal A et al. Localization of chondrocyte precursors in periosteum. Osteoarthritis Cartilage 2001;9:215–223.
8 Tanaka T, Taniguchi Y, Gotoh K et al. Morphological study of recombinant human transforming growth factor beta 1-induced intramembranous ossification in neonatal rat parietal bone. Bone 1993;14:117–123.
9 Orwoll ES. Toward an expanded understanding of the role of the periosteum in skeletal health. J Bone Miner Res 2003;18:949–954.
10 Choi Y-S, Lim SM, Shin H-C et al. Chondrogenesis of human periosteum-derived progenitor cells in atelocollagen. Biotechnol Lett 2007; 29:323–329.
11 Yu Z, Geng J, Gao H, Zhao X, Chen J. Evaluations of guided bone regeneration in canine radius segmental defects using autologous periosteum combined with fascia lata under stable external fixation. J Orthop Traumatol 2015;16: 133–144.
12 Wagner W, Wein F, Seckinger A et al. Comparative characteristics of mesenchymal stem cells from human bone marrow, adipose tissue, and umbilical cord blood. Exp Hematol 2005;33:1402–1416.
13 Pittenger MF, Mackay AM, Beck SC et al. Multilineage potential of adult human mesenchymal stem cells. Science 1999;284:143–147.
14 Ferretti C, Mattioli-Belmonte M. Periosteum derived stem cells for regenerative medicine proposals: Boosting current knowledge. World J Stem Cells 2014;6:266–277.
15 Stich S, Loch A, Leinhase I et al. Human periosteum-derived progenitor cells express distinct chemokine receptors and migrate upon stimulation with CCL2, CCL25, CXCL8, CXCL12, and CXCL13. Eur J Cell Biol 2008;87:365–376.
16 Hutmacher DW, Sittinger M. Periosteal cells in bone tissue engineering. Tissue Eng 2003;9((suppl 1)):S45–S64.
17 Tang KH, Dai YD, Tong M et al. A CD90(+) tumor-initiating cell population with an aggressive signature and metastatic capacity in esophageal cancer. Cancer Res 2013;73:2322–2332.
18 Takushima A, Kitano Y, Harii K. Osteogenic potential of cultured periosteal cells in a distracted bone gap in rabbits. J Surg Res 1998;78:68–77.
19 Chung MT, Liu C, Hyun JS et al. CD90 (Thy-1)-positive selection enhances osteogenic capacity of human adipose-derived stromal cells. Tissue Eng Part A 2013;19:989–997.
20 Yamamoto M, Nakata H, Hao J et al. Osteogenic potential of mouse adipose-derived stem cells sorted for CD90 and CD105 in vitro. Stem Cells Int 2014;2014:1–17.
21 Park B-W, Hah Y-S, Kim DR et al. Vascular endothelial growth factor expression in cultured periosteal-derived cells. Oral Surg Oral Med Oral Pathol Oral Radiol Endod 2008;108:554–560.
22 Ueno T, Kagawa T, Fukunaga J et al. Evaluation of osteogenic/chondrogenic cellular proliferation and differentiation in the xenogeneic periosteal graft. Ann Plast Surg 2002;48:539–545.
23 Park BW, Hah YS, Kim DR et al. Osteogenic phenotypes and mineralization of cultured human periosteal-derived cells. Arch Oral Biol 2007;52:983–989.
24 Wang P, Xie F, Pan J et al. Differences in the structure and osteogenesis capacity of the periosteum from different parts of minipig mandibles. J Oral Maxillofac Surg 2012;70:1331–1337.
25 Fan W, Crawford R, Xiao Y. Structural and cellular differences between metaphyseal and diaphyseal periosteum in different aged rats. Bone 2008;42:81–89.
26 Nakajima R, Ono M, Hara ES et al. Mesenchymal stem/progenitor cell isolation from tooth extraction sockets. J Dent Res 2014;93: 1133–1140.
27 Nakahara H, Goldberg VM, Caplan AI et al. Culture expanded periosteal-derived cells exhibit osteochondrogenic potential in porous calcium phosphate ceramics in vivo. Clin Orthop Relat Res 1990;276276–291.
28 Deschaseaux F, Sensébé L, Heymann D. Mechanisms of bone repair and regeneration. Trends Mol Med 2009;15:417–429.
29 Lim SM, Choi YS, Shin HC et al. Isolation of human periosteum-derived progenitor cells using immunophenotypes for chondrogenesis. Biotechnol Lett 2005;27:607–611.
30 De Bari C, Dell'Accio F, Vanlauwe J et al. Mesenchymal multipotency of adult human periosteal cells demonstrated by single-cell lineage analysis. Arthritis Rheum 2006;54:1209–1221.
31 Kawamoto K, Konno M, Nagano H et al. CD90− (Thy-1−) high selection enhances reprogramming capacity of murine adipose-derived mesenchymal stem cells. Dis Markers 2013;35:573–579.
32 Williams AF, Gagnon J. Neuronal cell Thy-1 glycoprotein: Homology with immunoglobulin. Science 1982;216:696–703.
33 Saalbach A, Kraft R, Herrmann K et al. The monoclonal antibody AS02 recognizes a protein on human fibroblasts being highly homologous to Thy-1. Arch Dermatol Res 1998;290:360–366.
34 McKenzie JL, Fabre JW. Human thy-1: Unusual localization and possible functional significance in lymphoid tissues. J Immunol 1981;126: 843–850.
35 McKenzie JL, Fabre JW. Distribution of Thy-1 in human brain: Immunofluorescence and absorption analyses with a monoclonal antibody. Brain Res 1981;230:307–316.
36 Rege TA, Hagood JS. Thy-1 as a regulator of cell-cell and cell-matrix interactions in axon regeneration, apoptosis, adhesion, migration, cancer, and fibrosis. FASEB J 2006;20:1045–1054.
37 Wiesmann A, Bühring HJ, Mentrup C et al. Decreased CD90 expression in human mesenchymal stem cells by applying mechanical stimulation. Head Face Med 2006;2:8.
38 Chen XD, Qian HY, Neff L et al. Thy-1 antigen expression by cells in the osteoblast lineage. J Bone Miner Res 1999;14:362–375.
39 Hosoya A, Hiraga T, Ninomiya T et al. Thy-1-positive cells in the subodontoblastic layer possess high potential to differentiate into hard tissue-forming cells. Histochem Cell Biol 2012; 137:733–742.
40 Chen XD, Qian HY, Neff L et al. Thy-1 antigen expression by cells in the osteoblast lineage. J Bone Miner Res 1999;14:362–375.
41 Dominici M, Le Blanc K, Mueller I et al. Minimal criteria for defining multipotent mesenchymal stromal cells. The International Society for Cellular Therapy position statement. Cytotherapy 2006;8:315–317.